System Identification of Building Structures with Continuous Modeling

RUICHONG ZHANG, FADI SAWAGED AND LOTFI GARGAB
Department of Civil & Environmental Engineering
Colorado School of Mines
1500 Illinois St. Golden, Colorado 80401
UNITED STATES OF AMERICA
rzhang@mines.edu http://inside.mines.edu/Zhang

Abstract: - This paper introduces a wave-based approach for system identification of high-rise building structures with a pair of seismic recordings, which can be used to evaluate structural integrity and detect damage in post-earthquake structural condition assessment. The fundamental of the approach is based on wave features of generalized impulse and frequency response functions (GIRF and GFRF), i.e., wave responses at one structural location to an impulsive motion at another reference location in time and frequency domains respectively. With a pair of seismic recordings at the two locations, GFRF is obtainable as Fourier spectral ratio of the two recordings, and GIRF is then found with the inverse Fourier transformation of GFRF. With an appropriate continuous model for the structure, a closed-form solution of GFRF, and subsequent GIRF, can also be found in terms of wave transmission and reflection coefficients, which are related to structural physical properties above the impulse location. Matching the two sets of GFRF and/or GIRF from recordings and the model helps identify structural parameters such as wave velocity or shear modulus. For illustration, this study examines ten-story Millikan Library in Pasadena, California with recordings of Yorba Linda earthquake of September 3, 2002. The building is modeled as piecewise continuous layers, with which GFRF is derived as function of such building parameters as impedance, cross-sectional area, and damping. GIRF can then be found in closed form for some special cases and numerically in general. Not only does this study reveal the influential factors of building parameters in wave features of GIRF and GRFR. It also shows some system-identification results, which are consistent with other vibration- and wave-based results. Finally, this paper discusses the effectiveness of the proposed model in system identification.

Key-Word: - Wave-based approach, Seismic responses of buildings, Wave propagation in structures.

1 Introduction

For performance-based structural design, vibration control, and damage diagnosis of high-rise structures such as ten-story Millikan Library in Fig. 1, response analysis and system identification are fundamental and typically carried out with a discrete, multi-degree-of-freedom (MDOF) model. As far as one-dimensional (1D) horizontal motion is concerned for example, the ten-story building can be modeled as a 10-DOF system with each floor mass and inter-story stiffness (i.e., physical parameters) calculable based on design configuration and materials, which can be calibrated in terms of identified vibratory features (i.e., modal frequencies, damping and shapes – a function of physical parameters) through Fourier spectral analysis of 11-set recordings of Yorba Linda earthquake of September 3, 2002 in Fig. 2. Subsequently, seismic demand such as structural peak acceleration to a scenario earthquake is predictable, which is useful for seismic design/retrofit and vibration control. Similarly, change of some physical parameters or higher-order modal parameters are identifiable with 11-set recordings of a new earthquake, which is detection and quantification of local, minor damage in post-earthquake structural condition evaluation.

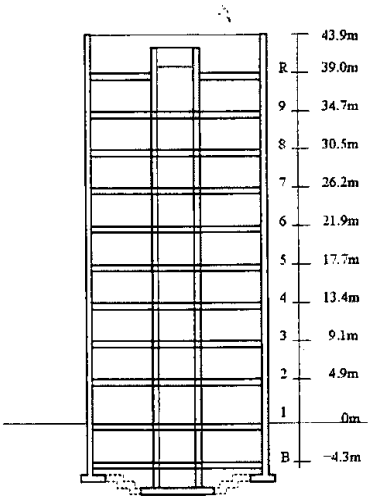

Fig. 1 Vertical cross section of the 10-story Millikan Library, Pasadena, California.

Furthermore, implementing damage mechanism such as material hysteresis, plastic hinge, and crack into the linear 10-DOF model would make the modeling rigorous in simulating nonlinear vibratory features, thus enhancing credibility in forward predicting analysis and inverse system identification, among many other broad-based applications.

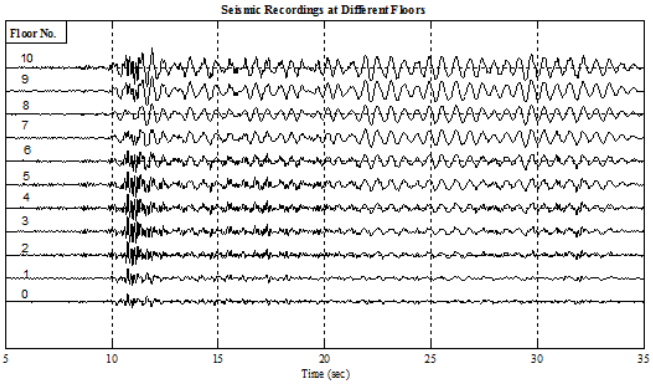

Fig. 2 Seismic acceleration recordings of Yorb Linda earthquake in the north-south direction at different floors (indicated as 0-10), where floor levels 0 and 10 correspond to B and R respectively in Fig. 1.

While the aforementioned vibration-based (or discrete-modeling-based) approach is overwhelmingly used in structural engineering, it has theoretical drawback – implicit assumption of *synchronous* motion at different heights – which distorts time-space characterization of seismic motion in buildings. For illustration, seismic responses obtained with the 10-DOF model will never show authentic floor-to-floor propagation features of high-frequency, dominant-energy waves, observed prominently in the 10-12.5s time window in Fig. 2. In other words, the vibration-based approach captures major motion features as function of time and distorts floor-to-floor motion relationship or wave features. Note that modal shapes essentially characterize floor-to-floor motion relationship of modified seismic responses with re-aligned time, thus not the true wave features. The wave-propagation features are even clearly exposed in the floor-to-floor time shift of the first peak motion in 0-0.2s time window in Fig. 3, which depicts pure structural acceleration responses at selected floors to a band-limit impulsive acceleration at basement (floor 0), extracted from recordings in Fig. 2 with the use of seismic interferometry or SI [1] by removing influences of seismic input and soil-structure interaction. For convenience, the pure response is referred here to as wave-based or generalized impulse response function or GIRF (to be elaborated).

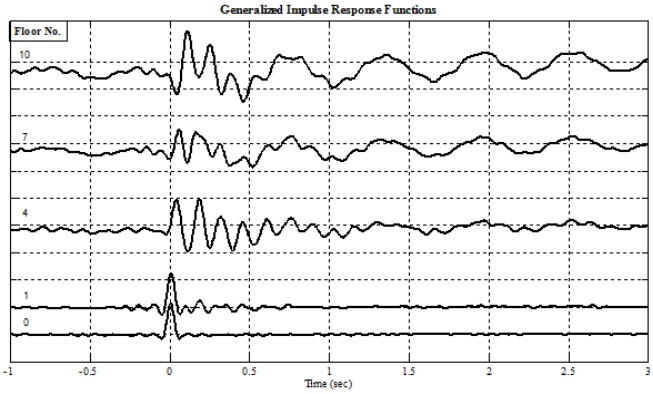

Fig. 3 GIRFs at selected floors with respect to band-limited impulsive basement acceleration.

Distorting the aforementioned wave features would falsely predict, likely underestimate, the maximum inter-story drift, a key index of seismic demand for structural design. This is due to the fact that time-delay peak waves at two neighboring stories would have the drift calculated as difference between one peak amplitude and one non-peak value, which is typically larger than the difference between two peak values without time-delay effect. Similarly, this time-delay feature would also affect the efficacy of vibration control, if actuators installed in different floors are operated with a central feedback-control device.

More important, understanding and utilizing the wave features could create an alternative wave-based (or continuous-modeling-based) approach for system identification of high-rise buildings, which can be used to improve greatly the efficiency of post-earthquake structural condition assessment, in comparison with traditional, vibration-based approach.

As well known, effectiveness of vibration-based system identification in general, and recognition of local physical parameters in particular, relies on a large number of recordings exemplified as 11-set recordings for Millikan Library, which is neither common nor practical for most structures currently or in the near future. In contrast, wave-based approach requires only a few of recordings. Take the building again as an example. For three available recordings at basement, the 4th and 7th floors, pure structural responses or GIRFs at the 4th and 7th floors are obtainable, as shown in Fig. 3. Then, the 1st peak-to-peak wave traveling time from the 4th to 7th floor is measurable, which is directly related to wave velocity of the building segment. Similarly, the corresponding peak-amplitude reduction is associated with the segment damping. Both identified velocity and damping can then be related to local physical parameters such as shear modulus and hysteretic damping if the building segment is modeled as a uniform shear-beam.

Indeed, recent studies also show advantages of wave-based approach over vibration-based one in some seismic response analysis and damage diagnosis of buildings. In particular, recognizing deficiency of discrete modeling in addressing seismic drift demand for buildings, Iwan in 1996 proposed to use 1D uniform shear-beam model for buildings and obtained seismic drift spectrum for design [2]. Inspired by Iwan's study and also from research in other disciplines, Safak in 1999 introduced 1D continuous modeling for structure-soil system with impulsive seismic excitation in bedrock [3]. With the model, he solved for wave responses with time-domain analysis methodology, compared them with MDOF structural modeling with ground excitation, and revealed wave propagation features and influences of soil-structure interaction in seismic structural responses, among others. Independently, Todorovska et al. in 2001 modeled 2D anisotropic wave propagation for a real seven-story building [4]. While developed over the past decade for exploration seismology, ultrasound and hazard studies, SI was first employed by Snieder et al. in 2006 to extract pure structural responses from seismic recordings, as shown in Fig. 3 [1],[5]. This SI methodology was not only used well for explaining wave phenomena in buildings, but also easily for system identification with a 1D uniform shear-beam model. Following Snieder's work, Kohler et al. in 2007 studied seismic propagating waves in 3D steel, moment-frame building and verified with ETABS finite-element modeling [6]. Recently, SI was further applied for damage detection based on 1D wave traveling times [7] and for seismic response analysis with continuous-discrete building models [8],[9], among others.

Building upon the aforementioned advances and others in relevant journals and proceedings such as a series of conferences in Structural Health Monitoring, e.g., Chang in 2009 [10] and Strong Motion Instrumentation Program (e.g., SMIP09 Seminar in 2009), this study proposes one-dimensional piecewise continuous modeling for wave propagation in building structures and examines its effectiveness in system identification.

2 Wave Propagation with Piecewise Continuous Building Model

In this study, a high-rise building is modeled as piecewise layered media shown in Fig. 4, each of which is characterized with shear wave speed $v = \sqrt{G/\rho}(1 + i\gamma\,\mathrm{sgn}(\omega))$ where G, ρ and γ are respectively equivalent shear modulus, mass density, and hysteretic damping ratio for the layer with cross-sectional area A and height h, i is imaginary unit, and $sgn(\omega)$ is the sign of frequency ω.

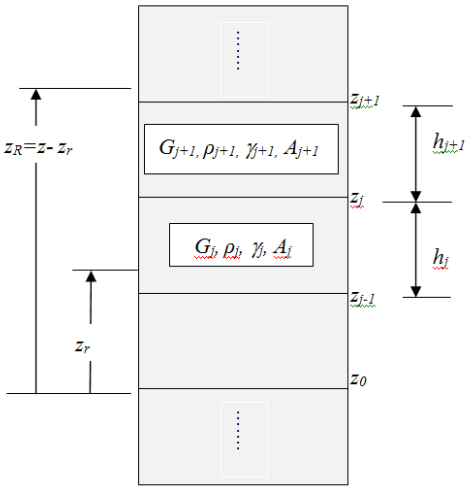

Fig. 4 A piecewise-continuous model for an N-layer building subjected to seismic motion below z_0.

Wave motion of shear displacement $u(z,t)$ in the j^{th} layer is governed by

$$\frac{\partial^2 u(z,t)}{\partial z^2} = \frac{1}{v_j^2}\frac{\partial^2 u(z,t)}{\partial t^2} \tag{1}$$

with displacement and force continuities at the j^{th} boundary as

$$u(z_j,t) = u(z_j^-,t), \quad G_{j+1}A_{j+1}\frac{\partial u(z_j,t)}{\partial z} = G_j A_j \frac{\partial u(z_j^-,t)}{\partial z} \tag{2a,b}$$

and a free boundary at the top

$$G_h A_h \frac{\partial u(z_h,t)}{\partial z} = 0 \tag{2c}$$

where superscript $^-$ indicates the negative side of the height z_j.

With Fourier transform

$$u(z,t) = \int_{-\infty}^{\infty} U(z,\omega)e^{i\omega t}d\omega, \quad U(z,\omega) = \frac{1}{2\pi}\int_{-\infty}^{\infty} u(z,t)e^{-i\omega t}dt \tag{3a,b}$$

one can solve Eqs. (1) and (2) for wave representation in frequency domain (ω) at z and wave-state relationship at z_l and z_m as

$$U_z = U(z,\omega) = U_z^u + U_z^d = C_1 e^{-i\omega z/v_j} + C_2 e^{i\omega z/v_j} \tag{4}$$

$$\begin{Bmatrix} U_m^u \\ U_l^d \end{Bmatrix} = \begin{bmatrix} T_{ml} & R_{lm} \\ R_{ml} & T_{lm} \end{bmatrix} \begin{Bmatrix} U_l^u \\ U_m^d \end{Bmatrix} \tag{5}$$

where displacement U_z consists of up-going and down-going waves denoted with superscripts u and d respectively, and transmission and reflection coefficients T_{ml} and R_{lm} (T_{lm} and R_{ml}) relate the outgoing waves U_m^u and U_l^d to input waves U_l^u and U_m^d for building segment bounded with (z_l,z_m), as seen in Fig. 5.

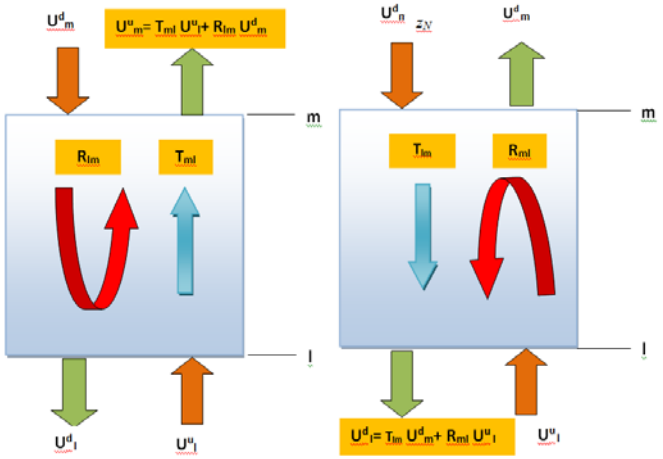

Fig 5a,b Transmission and refection coefficients T_{ml} and R_{lm} (Fig. 5a, left) or T_{lm} and R_{ml} (Fig. 5b, right) relate the out-going wave U_m^u (left) or U_l^d (right) and input waves U_m^d and U_l^u in building segment bounded by (z_l,z_m) or (l,m)

For the j^{th} layer bounded with (z_{j-1},z_j^-) and j^{th} boundary with (z_j^-,z_j), coefficients T and R can be found respectively as

$$T_{j^-(j-1)} = T_{z_j^- z_{j-1}} = e^{-i\omega h_j / v_j} = T_{(j-1)j^-}, \quad R_{j^-(j-1)} = R_{(j-1)j^-} = 0 \tag{6}$$

$$T_{jj^-} = \frac{2}{1+r_{I_j}}, \quad T_{j^-j} = T_{jj^-} r_{I_j}, \quad R_{jj^-} = T_{jj^-} - 1, \quad R_{j^-j} = T_{j^-j} - 1$$

$$r_{I_j} = \frac{\rho_{j+1} v_{j+1}}{\rho_j v_j} \frac{A_{j+1}}{A_j} \tag{7}$$

For the free building top, $\rho_{N+1}=v_{N+1}=A_{N+1}=0$ or $r_{I_N} = 0$, which degenerates Eq. (7) to $T_{NN^-} = 2$ and $R_{NN^-} = 1$, meaning that up-going wave $U_{N^-}^u$ is transmitted to the top with doubled amplitude and also reflected to down-going wave $U_{N^-}^d$ without changing the motion direction.

At the building lower end z_0 (or generally at referenced location z_r which could be selected as z_0), no segments below level z_0 are clearly specified in the model, yielding $r_{I_1} = 0$. One can then find $T_{0^-0} = 0$ and $R_{0^-0} = -1$, suggesting down-going wave U_0^d is completely reflected to the up-going wave U_0^u with the change of motion direction. While this feature will not be used in subsequent response calculation, it can help interpret wave phenomena at lower end z_0 with a fixed boundary.

For a composite building segment bounded with (z_l,z_n), or simply (l,n), with intermediate location z_m ($z_l<z_m<z_n$) such as (z_{j-1},z_j) with z_j^-, repeat use of Eq. (5) for (l,m) and (m,n) will lead to the representation of transmission and reflection coefficients in (l,n) in terms of those in two sub-segments in (l,m) and (m,n) as

$$T_{ln} = \frac{T_{lm} T_{mn}}{1 - R_{nm} R_{lm}}, \qquad R_{ln} = R_{mn} + \frac{T_{nm} R_{lm} T_{mn}}{1 - R_{nm} R_{lm}} \tag{8}$$

The above composition rule can be applied reversely for (n,l) and also repeatedly to find all the transmission and reflection coefficients between any two locations.

With the aforementioned coefficients R and T, wave response at z (or z_R=z-z_r) can then be related to those at referenced level z_r as

$$D_{Rr}(\omega) = \frac{U_{z_R}}{U_{z_r}} = \frac{(1 + R_{NR}) T_{Rr}}{(1 - R_{rR} R_{NR})(1 + R_{Nr})}$$

$$d_{Rr}(t) = \frac{1}{2\pi} \int_{-\infty}^{\infty} D_{Rr} e^{i\omega t} d\omega \tag{9a,b}$$

Equation (9a) indicates that D_{Rr} is dependent only upon R and T above z_r which are function of building properties in frequency domain. Wave response representation in general, and displacement response at z to an input displacement at z_r in particular, is then found as

$$u(z,t) = \int_{-\infty}^{\infty} D_{Rr} U_{z_r} e^{i\omega t} d\omega = \int_{-\infty}^{\infty} d_{Rr}(t-\tau) u(z_r, \tau) d\tau \tag{10}$$

which has the same mathematical form as traditional vibration response representation (e.g., Duhamel's or convolution integral) in frequency domain with D_{Rr} as frequency response function and in time domain with d_{Rr} as impulse response function. Because of the wave features with current continuous modeling, D_{Rr} and d_{Rr} are referred to respectively as wave-based or generalized frequency response function (GFRF) and generalized impulse response function (GIRF).

3 System Identification of Millikan Library with A Pair of Recordings

For illustration, this study shows parametric identification of the Millikan Library with the use of piecewise continuous model and a pair of seismic recordings after the Yorba Linda earthquake of September 3, 2002.

3.1 Wave and Vibration Features with Two-Layer Model

To show the wave-based approach for system identification different from vibration-based one, one can first examine a simple, two-layer model, which leads Eq. (9a) to

$$D_{R0}=\frac{[1+\alpha(e^{-2i\omega(\tau_1-\tau_z)}+e^{-2i\omega\tau_2})+e^{-2i\omega(\tau-\tau_z)}]e^{-i\omega\tau_z}}{1+\alpha[e^{-2i\omega\tau_1}+e^{-2i\omega\tau_2}]+e^{-2i\omega\tau}} \quad (11a)$$

$$0\le z\le h_1,\quad \tau_z=\frac{z}{v_1}$$

$$D_{R0}=\frac{2[1+e^{-2i\omega(\tau-\tau_z)}]e^{-i\omega\tau_z}/[1+r_{I1}]}{1+\alpha[e^{-2i\omega\tau_1}+e^{-2i\omega\tau_2}]+e^{-2i\omega\tau}}$$

$$h_1\le z\le h_1+h_2 \quad (11b)$$

$$\tau_z=\frac{h_1}{v_1}+\frac{z-h_1}{v_2}$$

where τ_z is the flight time for waves traveling from referenced z_0 to response location z, and

$$\alpha=\frac{1-r_{I1}}{1+r_{I1}},\quad \tau_1=\frac{h_1}{v_1},\quad \tau_2=\frac{h_2}{v_2},\quad \tau=\tau_1+\tau_2 \quad (12)$$

The GIRF can be found by substituting GFRF of Eqs. (11a,b) into Eq. (9b), where the integration can be obtained in closed form with the method of residues for some special cases and numerically for general cases. Below are presented some special cases, which could help understand the characteristics of wave propagation in buildings and subsequently aid in system identification for general cases.

The denominator of Eqs. (11a,b), a function of the real variable ω, is treated as a function of variable y, which has an infinite number of poles y_j (j=1,2,..) in the upper half complex plane, namely

$$1+\alpha[e^{-2iy\tau_1}+e^{-2iy\tau_2}]+e^{-2iy\tau}=0$$

$$y_j=(\pm1+i\gamma_{eq})\omega_j \quad (13)$$

$$j=1,2...,\infty$$

For $\gamma_1=\gamma_2$ and $\tau_1=\tau_2$, it can be found that

$$\omega_{2j-1}=[(2j-1)\pi-\beta]/\tau$$

$$\omega_{2j}=[(2j-1)\pi+\beta]/\tau \quad (14)$$

$$\gamma_{eq}=\gamma_1=\gamma_2,\quad \alpha=\pm\cos\beta$$

The closed-form solution of GIRF with Eq. (9b) for r_{I1}=1, which could be, but not necessarily, the uniform or one-layer model, can be found as

$$d_{Rr}=\frac{4\pi}{\tau}\sum_{j=1}^{\infty}(-1)^{j+1}e^{-\gamma\omega_j(t-\tau_z)}\cos\omega_j(\tau-\tau_z)\sin(\omega_j t) \quad (15)$$

which is consistent with those obtained in uniform shear-beam model [1],[8],[9].

Equation (15) indicates that GIRF consists of infinite number of motion modes, each of which has exponentially decaying damping factor, modal shape with cosine factor, and sinusoidal motion with modal frequency ω_j. This is essentially the traditional vibration perspective for seismic motion in buildings, in which the fundamental modal frequency ω_1 (similar to higher-order modal frequencies) is interpreted as vibration feature of building's periodic horizontal motion. Since ω_1 corresponds to the fundamental period $T_1=4\tau$, it can also be viewed as four times of the wave traveling time through the building height, i.e., wave interpretation.

To further clarify the wave propagation features, one can look at the model-based GIRFs at two locations. With the Millikan Library as an example, one can model it as one soft-thin layer (h_2=*1.22 m*) over a rigid-thick layer (h_1=*46.98 m*) with r_{I1}=*0.04*, v_1=*345.18 m/s*, v_2=*10.32 m/s*, and $\gamma_1=\gamma_2$=*0.03*. The selection of the two-layer parameters is not only based on structural configuration as shown in Fig. 1, i.e., the top thin roof portion is much less rigid than those for each and every story consisting of the floor and its half columns above and below, the latter of which can be unified approximately as one uniform thick layer. It also plays a major role in simulating non-negligible seismic waves at second modal frequency identified from seismic recordings, to be elaborated later. Fig. 6 shows model-based GIRFs of acceleration at the 4th and 7th floors to an impulsive acceleration at basement (d_{40} and d_{70}), from which wave propagation with damping-related amplitude attenuation is clearly observed.

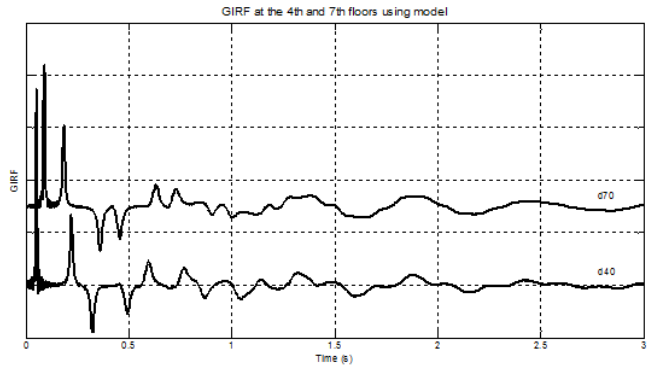

Fig 6 GIRFs at the 4th and 7th floors with respect to impulsive basement acceleration obtained based on Eqs. (10)-(12) with r_{I1}=*0.04*, v_1=*345.18 m/s*, v_2=*10.32 m/s*, h_1=*46.98 m*, h_2=*1.22 m*, and $\gamma_1=\gamma_2$=*0.03*.

In particular, the first peak of d_{40} is rooted from the impulse at the basement (level 0), which is propagated to the first peak of d_{70} with reduced amplitude. That first peak at the 7th floor is further propagated to the building top and then reflected to travel downward to the 7th and subsequently 4th floors, and generates the second peaks with further reduced amplitudes. The second peak at the 4th floor continues the downward propagation to the basement. Since the motion disappears at basement at $t\neq 0$ (due to impulse feature at basement which is proved as a fixed boundary), a negative, same-amplitude peak, balancing the positive one at the basement, is generated and propagated upward. That negative peak is propagated to the 4th and then 7th floors with sequentially-reduced amplitude (shown as the third, negative peaks in d_{40} and d_{70}), and continues with previous wave propagation pattern. As time goes on, wave response at the 7th floor (similar to the 4th floor) is then dominated by vibration character of a resonance for the whole building, which has fundamental period equal to 4τ, or four times of the wave traveling time through the building height. It is verified theoretically and numerically that the peak-to-peak time elapse (or simply flight time) between the two locations (or at one location with implicit other for free top) is the wave travelling time. It is also noted that wave reflection and transmission at connection of layers 1 and 2 do affect the wave amplitude reduction and flight time, which will be discussed later.

In short, the above shows wave and vibration features in GIRF and GFRF, also confirming the aforementioned clarification in terming the GIRF/GFRF, i.e., wave-based or generalized version of traditional IRF and FRF with discrete MDOF modeling.

3.2 Parametric Identification with Two-layer Model

For system identification, recording-based GFRF/GIRF is required. One can first calculate the recording-based GFRF as

$$\widetilde{D}_{j0}=\frac{\widetilde{U}_j\widetilde{U}_0^*}{|\widetilde{U}_0|^2+\varepsilon}\quad\underset{\varepsilon\to 0}{\Rightarrow}\quad\frac{\widetilde{U}_j}{\widetilde{U}_0} \tag{16}$$

where $\widetilde{U}$ is the recording in frequency domain, superscript asterisk indicates the complex conjugate, and ε is a positive small number, implying the added white noise. The white noise is used primarily to avoid unstable calculation of GFRF at some frequencies near the notches in the spectrum $\left|\widetilde{U}_0\right|^2$, as suggested in Snieder and Safak [1]. As ε approaches zero, $\widetilde{D}_{j0}(\omega)\Rightarrow\frac{\widetilde{U}_j}{\widetilde{U}_0}$, which is Fourier spectral ratio or the definition of GRFR in Eq. (9a). Note that the tilde over quantities D and U is used to distinguish the recording-based quantities from those based on modeling or Eqs. (9a) and (11a,b).

For a pair of recordings available at basement and floor 7, the GFRF of $\widetilde{D}_{70}$ with ε=5% of total power spectrum of basement motion can be found in Fig. 7. In principal, all the frequencies corresponding to the spectral peaks in Fig. 7 can be regarded as modal frequencies and then used for system identification. For simplicity in practice and also for illustration with the use of a two-layer model, parametric identification is carried out here based on two modal frequencies identified from Fig. 7 as ω_1=10.62 *rad/s* and ω_2=14.21 *rad/s*.

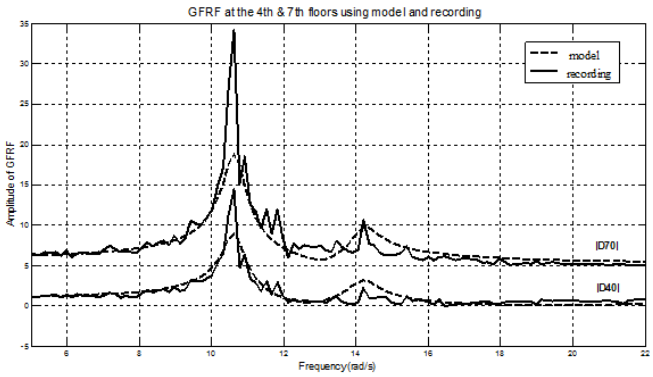

Fig. 7 Comparison of GFRF amplitudes at the 4th and 7th floors with respect to impulsive basement acceleration obtained from seismic recordings and model (Eq. (11a)).

With the use of Eqs. (14), the following two parameters are found

$$\tau=\frac{2\pi}{\omega_1+\omega_2},\quad \beta=\frac{\pi(\omega_2-\omega_1)}{\omega_1+\omega_2} \tag{17}$$

which yields τ=0.253 *s* and β=0.454 *rad*, and subsequently r_{11}=*0.053*, v_1=*361.85 m/s*, v_2=*19.18 m/s*, h_1=*45.77 m*, h_2=*2.43 m* with Eqs. (12) and (14). These identified parameters are quite close to the aforementioned, pre-selected ones based on structural configuration for Fig. 6. This partially confirms the appropriateness of the identification approach.

It should also be noted that the aforementioned identification is under special condition, i.e., $\gamma_1=\gamma_2$ and $\tau_1=\tau_2$. In general, parameters r_{11}, v_1, v_2, h_1 and h_2, together with γ_1 and γ_2, can be found by minimizing mean squared error of the model-based GFRF from recording-based GFRF in certain frequency range (say 5-22 *rad/s*), among many other identification algorithms. While it is doable, this study instead presents the

comparison of model-based GFRFs with the aforementioned, pre-selected parameters with recording-based ones, aiming to show the influences of some parameters in GFRF and GIRF. Fig. 7 and 8a,b show respectively the comparison of recording-based GFRF and GIRF at the 4th and 7th floors with respect to band-limited (ε=5%) impulsive motion at basement against model-based counterparts with respect to pure (ε=0%) impulsive motion at basement.

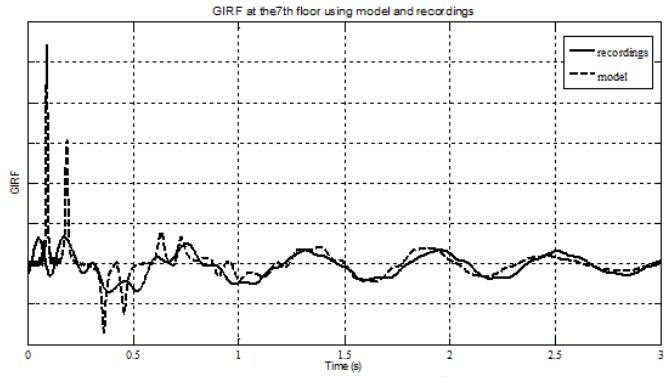

Fig 8a Comparison of GIRF at the 7th floors with respect to basement acceleration motion obtained from seismic recordings and model (Eqs. (9b) and (11a)).

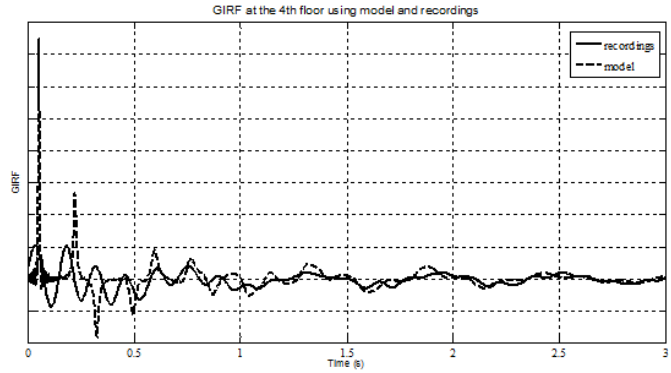

Fig. 8b Comparison of GIRF at the 4th floor with respect to basement acceleration motion obtained from seismic recordings and model (Eqs. (9b) and (11a)).

These three figures indicate that the two-layer model is able to capture the fundamental wave and vibration features shown in the recordings, exemplified as the first and second modal frequencies in Fig. 7, and proximity of first couples of wave arrival times and well-matched resonant vibration features in Figs. 8a,b. The major difference in spectral amplitudes at the first modal frequency in Fig. 7 and in wave amplitude and arrival time in the 0-0.5 *s* time window in Figs. 8a,b can be minimized with appropriate system-identification algorithm for identifying layer parameters and ε.

3.3 Influences of Multi-layer Model in Parametric Identification

While some fundamental characteristics of wave-based system identification are shown with the two-layer model, increased number of layers in the model would be in principle more appropriate in realistically capturing the physical multi-story structure of the building. To see the influence of multi-layer model in system identification, one can alternatively examine the difference of GFRF and GIRF with two-layer and 11-layer models. Based on the structural configuration in Fig. 1, the building can be modeled as 11 layers, with the top 11th layer being the same as the 2nd layer in the 2-layer model, and with the first ten layers having same flight time as the first layer in the 2-layer model. Due to the story-to-story proximity in structure in Fig. 1, the flight time for the first 10 layers is assumed to be equally shared with each of ten layers in 11-layer model. The minor difference in story height in Fig. 1 then leads to slightly-different velocity in each layer and $r_{lj}\approx 1$ for j=1-10. This yields

$T_{jj^-} \approx T_{j^-j} \approx 1, \quad R_{j^-j} \approx R_{jj^-} \approx 0, \quad for \quad j = 1-10$ and

$T_{ln} \approx T_{lm}T_{mn}, \quad R_{ln} \approx R_{mn}, \quad for \quad l,m = 1-10$ with the aid of Eqs. (7) and (8), and subsequently leads to the *T*s and *R*s in the first ten layers in 11-layer model similar to those with first layer in 2-layer model. With those *T*s and *R*s, GFRF with the 11-layer model obtained from Eq. (9a) with N=11 is essentially similar to Eqs. (11a,b) with two-layer model.

Figure 9 shows that both 2-layer and 11-layer models with Table 1 are consistent to each other in GFRF, in addition to capturing the two modal frequencies.

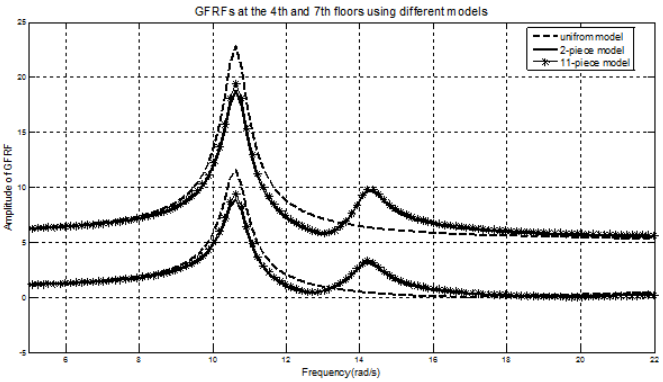

Fig. 9 Comparison of GFRF amplitudes at the 4th and 7th floors with respect to impulsive basement acceleration obtained with uniform (one-layer), two-layer and eleven-layer models from seismic recordings and models.

Table 1 Identified shear wave speeds and damping and their comparison with results from others, which are

associated with uniform, one-layer model with a pair of Yorb Linda earthquake recordings at basement and the 8th floor [9] and with 11-set recordings of the same earthquake shown in Fig. 2 [1], and Table 11.1.1 in Chopra [11] with Lytle and San Fan Fernando earthquake recordings respectively.

Table 1: Yorb Linda Earthquake recordings

	ω_1 and ω_2 (rad/s)	Wave Speed, height	Damping
w/ Lytle EQ (w/ San Fan Fernando EQ)	12.08 (10.13) 52.36 (48.33)		0.029 0.064
One-layer model from Zhang et al. 2011 (identified data from Snider and Safak 2006)	10.77	v=330 m/s, h=48.2 m (322 m/s)	0.0187 (0.0244)
2-layer model	10.77 14.21	v_1=345 m/s, h_1=47 m v_2=10 m/s, h_2=1.2 m	γ_1=0.03 γ_2=0.03
11-layer model	10.77 14.21	$v_j=h_j/\tau_j$, τ_j=0.0136 s, h_j is obtained with Fig. 1 as j=1-9, h_{10}=7.98 m, v_{11}=10 m/s, h_{11}=1.2 m	γ_j=0.03 j=1-11

On the other hand, wave and vibration features in GFRF and GIRF with uniform one-layer model is qualitatively different from those in 2- or 11-layer model, for the former cannot capture the motions with the second modal frequency, as shown in Fig. 9. The difference can also be seen in Fig. 10, although it is not as qualitatively clear as in Fig. 9.

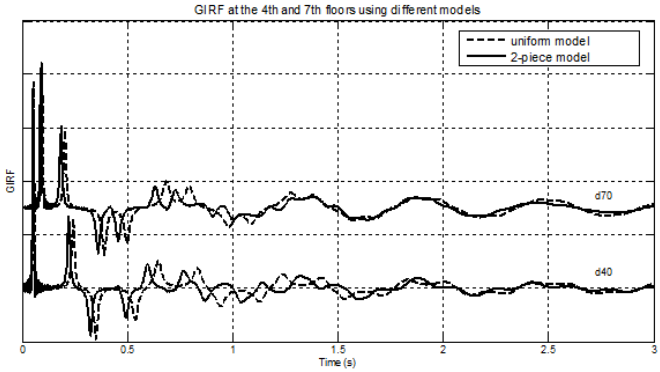

Fig. 10 Comparison of GIRFs at the 4th and 7th floor with respect to impulsive basement acceleration obtained with one- and two-layer models.

In summary, the presented analysis suggests that two-layer model is effective in system identification for buildings structures like Millikan Library in general, and in improved accuracy in capturing higher-order wave motions in particular. The increased number of layers in the modeling is not essentially helpful in capturing fundamental wave features. It could nevertheless be useful in system identification with non-uniform structure in height.

3 CONCLUSION

This study proposes piecewise continuous modeling for seismic wave motion in high-rise structures. It first derives the generalized impulse and frequency response functions (GIRF and GFRF) which are fundamentally important in constructing response to the motion input to a system, not the traditional force input. The features of GIRF and GFRF as well as seismic responses are also examined in detail, revealing not only well-observed vibration features of building structures, but also some perspective of seismic wave behaviors of structures which traditional vibration-based approach does not show clearly. The proposed model can then be used for system identification of building structures, exemplified with Millikan Library with two-layer model. Results show the proposed approach is efficient.

While this study focuses on system identification, it can be easily extended for damage diagnosis in post-earthquake conditional assessment for a pair of available recordings of an earthquake, which is the subject of future study.

5 ACKNOWLEDGMENT

This work was supported by the Colorado School of Mines – Petroleum Institute joint research project under the auspices of Abu Dhabi National Oil Company. The opinions, findings and conclusions expressed herein are those of the authors and do not necessarily reflect the views of the sponsors.

References :

[1] Snieder R. and Safak E., Extracting the building response using seismic interferometry: Theory and application to the Millikan library in Pasadena, California, *Bull. Seism. Soc. Am*. 2006, 96(2), 586-598.

[2] Iwan, W.D. (1996) "Drift spectrum: measure of demand for earthquake ground motions," *Journal of Engineering Mechanics-ASCE*, 123, 397-404.

[3] Safak E., Wave-propagation formulation of seismic response of multistory buildings, *Journal of Structural Engineering*, ASCE, 1999, 125(4), 426-437.

[4] Todorovska M.I., Ivanovic S.S., and Trifunac M.D., Wave propagation in a seven-story reinforced concrete building I: Theoretical

models, *Soil Dynamics and Earthquake Engineering*, 2001, 21, 211-223.

[5] Snieder R., Sheiman J., and Calvert R. Equivalence of virtual-source method and wave-field deconvolution in seismic interferometry, *Physical Review*, 2006, E73, 066620(9 pages).

[6] Kohler M.D., Heaton T.H., and Bradford S.C., Propagating waves in the steel, moment-frame Factor Building recorded during earthquakes, *Bull. Seism. Soc. Am*. 2007, **97**(4), 1334-1345.

[7] Todorovska, M.I. (2009) "Earthquake damage detection in buildings and early warning based on wave travel times," *Proceedings of 2009 NSF Engineering Research and Innovation Conference*, Hawaii.

[8] Zhang, R., S. Al Hilali, A. Abdulla, and M. Al Kurbi (2010) "A Wave-based Approach for Seismic Response Analyses of High-Rise Buildings," Proceedings of the IUTAM Symposium *(International Union for Theoretical and Applied Mechanics)*, Vol. 29, *Nonlinear Stochastic Dynamics and Control* (Zhu, Lin and Cai, eds.), 336-346, ISBN: 978-94-007-0731-3.

[9] Zhang, R., R. Snieder, L. Gargab and A. Seibi (2011) "Modeling of seismic wave motion in high-rise buildings," *Probabilistic Engineering Mechanics*, 26(4), 520-527.

[10] Chang, F.G. (2009). Structural Health Monitoring 2009. Technomic, Lancaster, PA.

[11] Chopra A. Dynamics of Structures-Theory and Applications to Earthquake Engineering, Prentice-Hall, Inc., 1995.